ISSN: 1692-7257 - Volume 1 – Issue 47 - 2026

ORIGINAL

RCTA
Revista Colombiana de Tecnologías de Avanzada
UNIPAMPLONA

Synthesis of nickel plates coated by electrodeposition with NixSy

Síntesis de placas de níquel recubiertas mediante electrodeposición con NixSy

Esteban Quintero Moreno[1,2]
Héctor Darío Sánchez Londoño[1]
Edwin García Quintero[1]

[1] **Universidad de Antioquia, Facultad de ingeniería, Grupo de investigación TESLA, Medellín, Antioquia, Colombia.**

[2] **ITM, Institución Universitaria, Facultad de Ciencias Exactas y Aplicadas, Departamento de Ciencias Básicas, Medellín, Antioquia, Colombia.**

Received: 12 November 2025. Revised: 30 November 2025. Accepted: 18 December 2025. Published: 09 February 2026.
Corresponding Author: Esteban Quintero Moreno

How to cite: E. Quintero Moreno, H. D. Sánchez Londoño, and E. García Quintero, "Síntesis de placas de níquel recubiertas mediante electrodeposición con NixSy", *Revista Colombiana de Tecnologías de Avanzada (RCTA)*, vol. 1, no. 47, feb. 2026, art. no. 4355, doi: 10.24054/rcta.v1i47.4355

This work is licensed under a Creative Commons Attribution-NonCommercial 4.0 International License.

Abstract:

The present article aims to analyze the current, voltage, and time parameters involved in the electrodeposition of nickel sulfide nanolayers on pure nickel plates through a synthesis route based on variations in the number of cycles (1, 3, 4, and 7). Each cycle consists of four different voltage steps within the range of 0.54–2.4 V, which are repeated according to the corresponding number of cycles. A nickel nitrate hexahydrate solution (0.05 mol/L) and sodium thiosulfate pentahydrate (0.1 mol/L) were used as the electrolyte. The voltage values exhibit high stability, with oscillations of ±0.2 V, indicating that the employed methods provide a high degree of control over the electrodeposition process. Additionally, a mass gain in the range of 0.44–6.57 mg was obtained for the electrodepositions.

Keywords: nanotechnology, electrodeposition, layer engineering, sulfur, nickel.

Resumen:

El presente artículo tiene como objetivo analizar los parámetros de corriente, voltaje y tiempo en la electrodeposición de nanocapas de sulfuro de níquel sobre placas de níquel puro mediante una vía de síntesis basada en variaciones del número de ciclos (1, 3, 4 y 7). Cada ciclo consta de cuatro escalones de voltaje diferentes en el rango de (0.54–2.4) V, los cuales se repiten de acuerdo con el número de ciclos correspondiente. Como electrolito se utilizó una solución de nitrato de níquel hexahidratado (0.05 mol/L) y tiosulfato de sodio pentahidratado (0.1 mol/L). Los valores de voltaje presentan una alta estabilidad, con oscilaciones de ±0.2 V, lo que indica que los métodos empleados permiten un elevado control sobre el proceso de electrodeposición. Adicionalmente, se obtuvo una ganancia de masa en el rango de (0.44–6.57) mg para las electrodeposiciones realizadas.

Palabras clave: nanotecnología, electrodeposición, ingeniería de capas, azufre, níquel.

INTRODUCTION

The planet faces constant challenges; a few years ago in 2023, we already exceeded six of the planetary limits [1], and it was theprevious year (2025)when we surpassed seven of the nine planetary boundaries [2], a worrying element is ocean acidification, as it puts the planet's marine life at risk. Many efforts are being directed in this regard, including finding alternative forms of energy production that are friendly to the planet and, in this regard, hydrogen production [3] using water electrolysis is a great tool [4], [5], [6], [7], for which we need to delve into the role of the electrodes used in the process [8] and how some doping on the electrodes helps improve the process [9], [10], [11], additionally, we found that NixSy electroplating on nickel plates is a very promising process [12], [13] for which we carry out the experimental design and characterize the deposited mass.

METHODOLOGY

Experimental design and factorial designs

The design and analysis of experiments allowed us to determine two central elements in the research: the first was that it allowed us to determine the determining variables of the synthesis that impact the layer thickness of the final sample, and the second allowed us to determine the number of samples needed and thereby optimize the total time of the experimental phase[14],[15].

For the research, we built a two-factor factorial design for synthesis I, the number of cycles and the voltage change ($\Delta V = V_{final} - V_{inicial}$); one cycle has a time of 4 min and consists of setting a different voltage value each minute. We made the decision to build a $4x3$ factorial (4 levels for cycles and 3 levels of ΔV) with one replicate and for two differentiated treatments, hereafter identified as "Synthesis I, Treatment I" and "Treatment II", which can be observed in the following figures respectively, Fig. 1 and Fig. 2; additionally, we present tables 1 and 2 with the respective values.

It is important to clarify that in the synthesis process the electrolyte has multiple factors such as concentration, temperature, agitation, among many others[16], therefore, the decision was made to preserve all these invariant factors throughout the experimental phase; we do this by following the same synthesis protocol without changing the electrolyte precursors; additionally, the configuration of the electrodeposition system remains invariant.

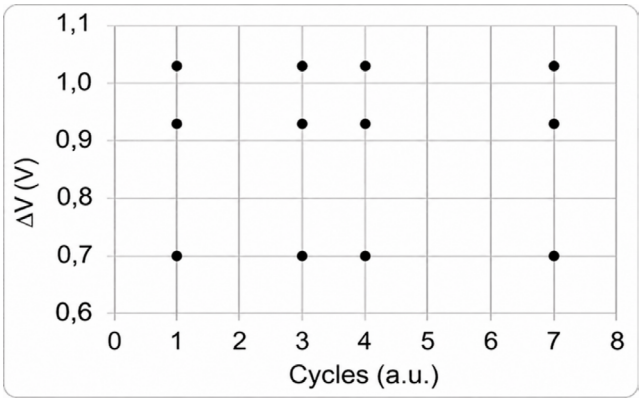

Fig. 1. Plot of the 4 x 3 factorial design, Synthesis I, Treatment I.

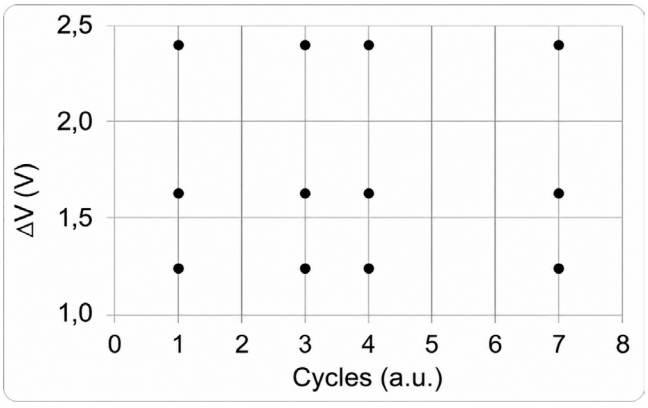

Fig. 2. Plot of the 4 x 3 factorial design, Synthesis I, Treatment II.

Table 1: Data from the plot of the 4×3 ***factorial design, Synthesis I, Treatment I.***

Cycles (a.u.)	V (V)
1	0.70 – 0.93 – 1.03
3	0.70 – 0.93 – 1.03
4	0.70 – 0.93 – 1.03
7	0.70 – 0.93 – 1.03

Table 2: Data from the plot of the 4×3 ***factorial design, Synthesis I, Treatment II.***

Cycles (a.u.)	V (V)
1	1.24 – 1.63 – 2.40
3	1.24 – 1.63 – 2.40
4	1.24 – 1.63 – 2.40
7	1.24 – 1.63 – 2.40

In the synthesis process, we decided to keep all these factors invariant for the entire experimental phase, which consists of 24 experiments, each with one replicate; the configuration of the electrodeposition system of Fig. 3 is also kept invariant.

The nickel electrode is a square sheet with an approximate area of $1\ cm^2$ and a few millimeters in thickness.

Data acquisition

The power supply for the electrodeposition was precisely regulated with a Wuzhi WZ5005 DC-DC voltage regulator, which has an input voltage range of $(6-55)\ VDC$ and output parameters of $(0-50)\ VDC$ and $(0-5)\ A$, with delivery accuracy of $0.01V$ and $0.001A$ for voltage and current, respectively.

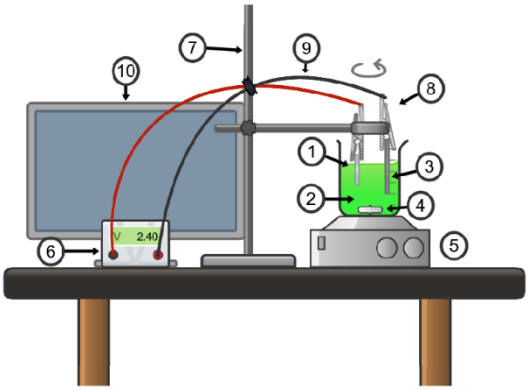

Fig. 3. *Electrodeposition system. 1. Nickel electrode. 2. Synthesis electrolyte. 3. Stainless steel electrode. 4. Magnetic stir bar. 5. Magnetic stirrer and heater. 6. Voltage or current source. 7. Vertical stand. 8. Clamps. 9. Cables. 10. Computer with software for data acquisition from the Arduino.*

Although the voltage regulator has a display, a voltage divider circuit connected in parallel with the positive and negative terminals was implemented, which allows the data to be stored.

Because current also has to be read, a Hall effect sensor was used. It was connected in series with the power supply circuit of the voltage regulator to the electrodeposition system.

Finally, for data acquisition and to program the sampling times, an Arduino Mega board was used, to which the sensors and reading circuits were connected through the analog ports, which have a 10-bit ADC module for $(0-5)\ VDC$ signals. The data were stored on a microSD card with the help of a "datalogger" which communicated with the Arduino via the SPI protocol, creating a .TXT file for statistical analysis.

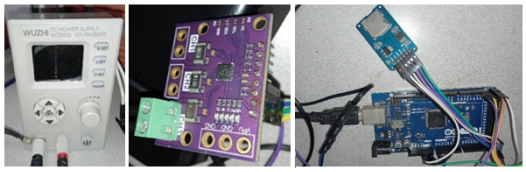

Fig. 4. *Top left: voltage regulator. Top right: Hall effect sensor. Bottom: "datalogger" and Arduino Mega.*

Synthesis

The synthesis experiments were carried out with $Ni(NO_3)_2{*}6H_2O$ $(0.05mol/l)$ and $Na_2S_2O_3{*}5H_2O$ $(0.1mol/l)$ with agitation by $10min$, as shown in Fig. 5, which correspond to 24 syntheses each with a replica presented in the Table 1, in which treatment I is identified, corresponding to cycles of 1, 3, 4, and 7 for voltages of $0.54-0.84-1.14-1.24\ V$ which correspond to series 1, then for the voltages of $0.7-0.92-1.17-1.63\ V$ which correspond to series 2 and then for the voltages of $1.37-1.68-1.94-2.4\ V$

which correspond to series 3; and treatment II, corresponding to series 1, 2, and 3, is also identified with an additional 4-minute cycle at the maximum voltage of each synthesis.

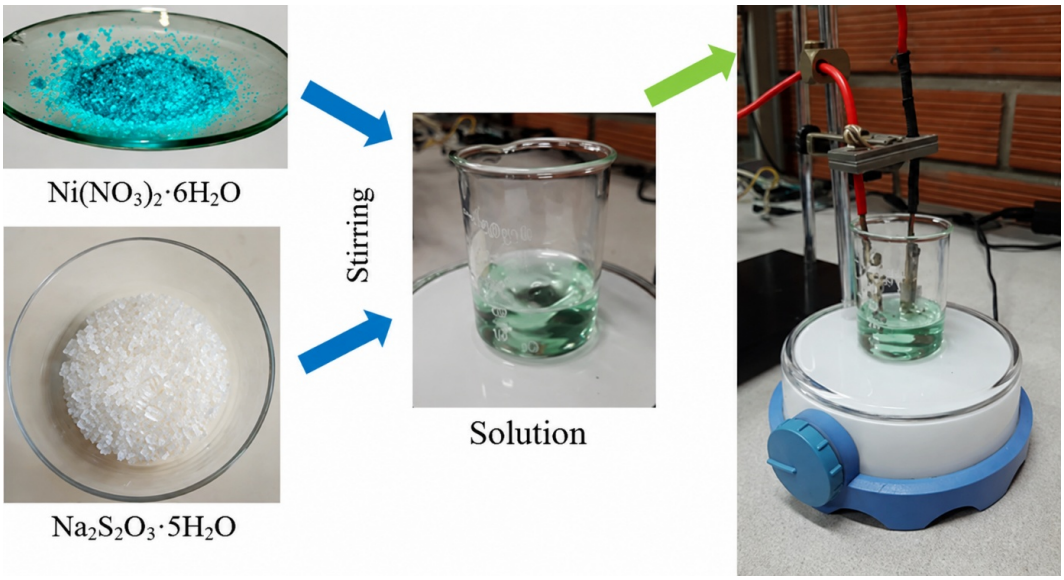

Fig. 5. *Synthesis scheme I.*

Table 1: Set of experiments carried out for the synthesis, including the sample label, the voltage supplied per minute and the number of cycles; first is treatment I and then treatment II, which corresponds to the additional cycle.

Treatment I			
Sample	Voltage (V)	Cycles	
1	0.54 – 0.84 – 1.14 – 1.24	1	
2		3	
3		4	
4		7	
5	0.7 – 0.92 – 1.17 – 1.63	1	
6		3	
7		4	
8		7	
9	1.37 – 1.68 – 1.94 – 2.4	1	
10		3	
11		4	
12		7	
Treatment II			
Sample	Voltage (V)	Cycles	Additional
13	0.54 – 0.84 – 1.14 – 1.24	1	4 minutes at 1.24 V
14		3	
15		4	
16		7	
17	0.7 – 0.92 – 1.17 – 1.63	1	4 minutes at 1.63 V
18		3	
19		4	
20		7	
21	1.37 – 1.68 – 1.94 – 2.4	1	4 minutes at 2.4 V
22		3	
23		4	
24		7	

It was decided to carry out this synthesis route after an analysis of different options [17], [18], [19], [20], [21].

RESULTS AND ANALYSIS

Synthesis

In the synthesis, two (2) treatments were developed, each with its own particularities, and these are developed and explained separately in Treatment I and Treatment II, respectively.

Treatment I

In Treatment I, three series of experiments were carried out, as follows:

Series 1: samples 1 to 4.

Series 2: samples 5 to 8.

Series 3: samples 9 to 12.

Series 1 has a voltage range of $0.7V$. In sample 1 (Fig. 6), as in its replicate, the current at the start of the synthesis shows an increase, that is, when the voltage is $0.54V$, and then decreases gradually during that first cycle. At the second voltage level, the current increases again, although this time at almost the same initial current value; at the third voltage level the current shows a larger increase followed by a decay; and finally, at the fourth voltage level, where we are at $1.24V$, the highest current peak of the entire synthesis is observed. This may be due to the increase in potential and to the passivation of the current at each of the levels, and may be due to the system incorporating layers of material onto the electrode, which decreases the current as time passes.

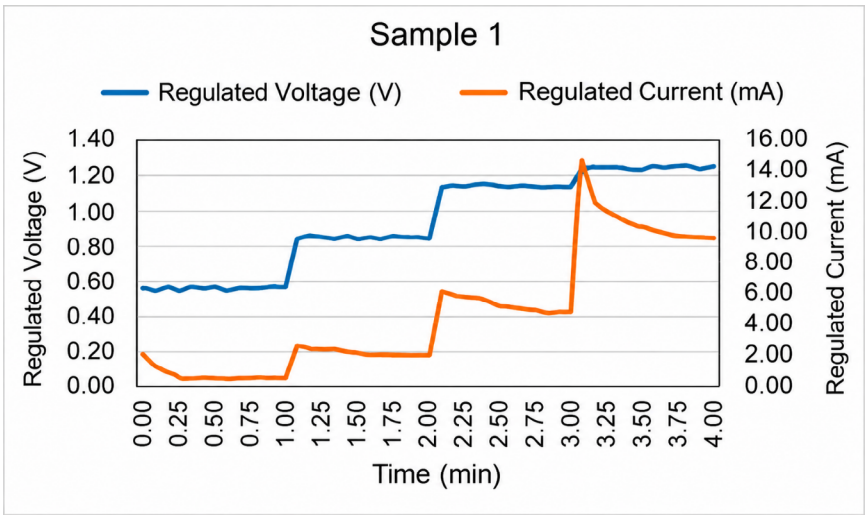

Fig. 6. *Sample 1, with one cycle, for four voltage levels.*

In sample 2 (Fig. 7), as in its replicate, during the three cycles the current shows a behavior similar to that of samples 1 and 1* with regard to the first cycle, but for the second cycle the current at the first voltage level is almost zero, which is repeated for the third cycle and is much more evident at the second level, which almost disappears, which may indicate a passivation of the electrode. In addition, the current peaks in the three cycles at voltage level four decrease in intensity, which points to stability of the system.

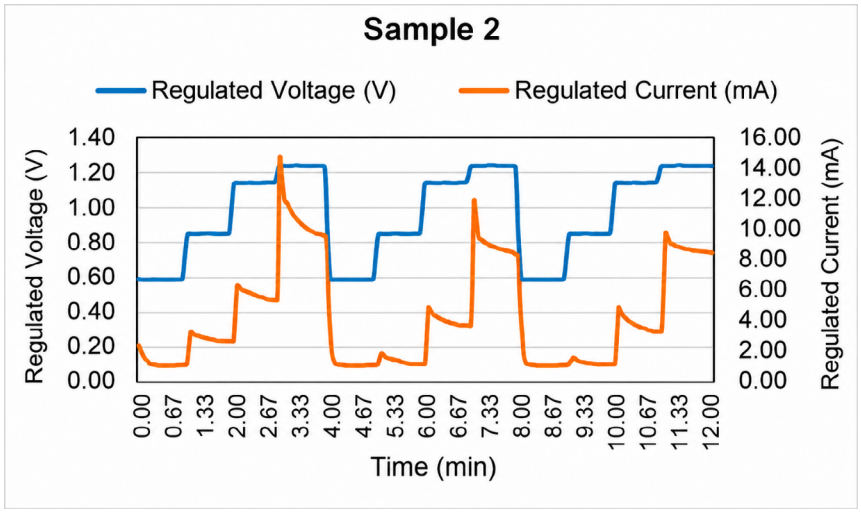

Fig. 7. *Sample 2, with three cycles, for four voltage levels.*

In sample 3 (Fig. 8), as in its replicate, for the fourth cycle the current at the first voltage level is practically nonexistent, as at the second voltage level; even so, for the third and fourth voltage levels in the fourth cycle a very stable system is evident, which may indicate a passivation of the electrode.

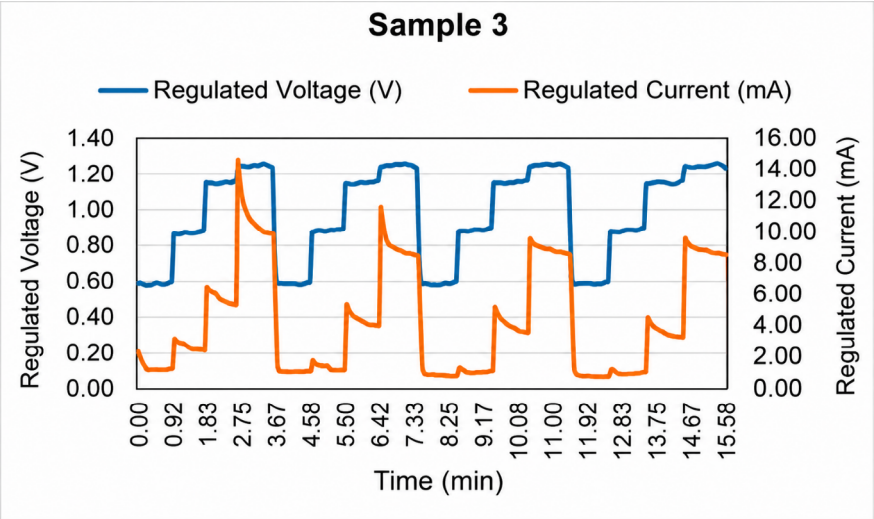

Fig. 8. *Sample 3, with four cycles, for four voltage levels.*

In sample 4 (Fig. 9), as in its replicate, for the fifth, sixth and seventh cycles the current at the first two voltage levels is almost zero; even so, for the third and fourth voltage levels, in the fifth, sixth and seventh cycles a very stable system is evident, with a slight increase in the current peak in the seventh cycle; this behavior is present from the third cycle onward.

The current peaks in samples 1, 2, 3 and 4 had values between $14.71mA$ and $8.63mA$.

Series 2 has a voltage range of $0.93V$; as for the current, it showed a behavior similar to that of the previous samples, except that it has current peaks at values of $20.02mA$ and $11.09mA$.

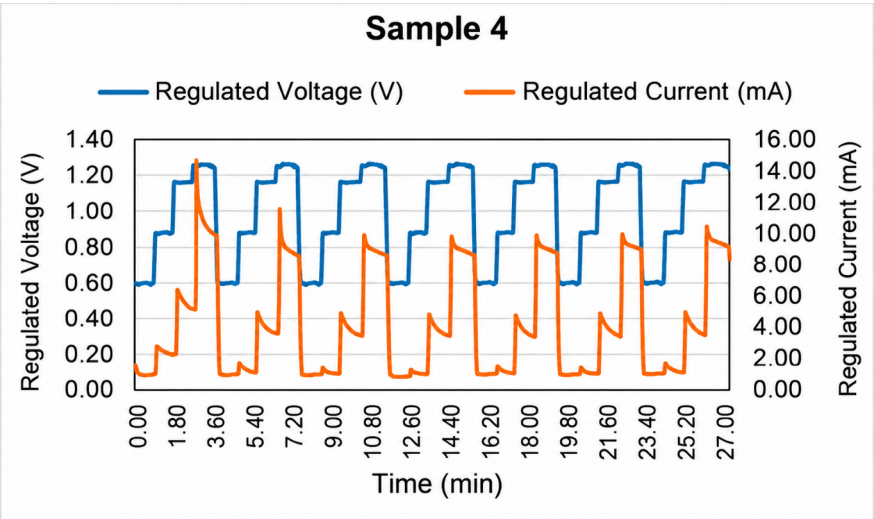

Fig. 9. *Sample 4, with seven cycles, for four voltage levels.*

Series 3 has a voltage range of $1.03V$; as for the current, it showed a behavior similar to that of the previous syntheses, except that it has current peaks at values of $28.22mA$ and $16.59mA$.

It should be added that the voltage behaved in a stable manner in all the experiments and for all the cycles.

Treatment II

In treatment II, three series of experiments were carried out, as follows:

Series 1: samples 13 to 16.

Series 2: samples 17 to 20.

Series 3: samples 21 to 24.

In samples 13, 14, 15 and 16 (Fig. 10) and their respective replicates samples 13*, 14*, 15* and 16*, the voltage behaved

stably in all experiments and for all cycles. The current showed a behavior similar to that of the previous syntheses, except that in the last cycle there was a stable current with a difference of $1mA$ for all samples.

In samples 17, 18, 19 and 20 (Fig. 11) and their respective replicates samples 17*, 18*, 19* and 20*, the current showed a behavior similar to that of the previous syntheses, except that in the last cycle there was a stable current with a difference of $1.95mA$ for all samples. The same behavior appeared in samples 21, 22, 23 and 24 (Fig. 12) and their respective replicates samples 21*, 22*, 23* and 24*, except that in the last cycle there was a stable current with a difference of $2.83mA$ for all samples.

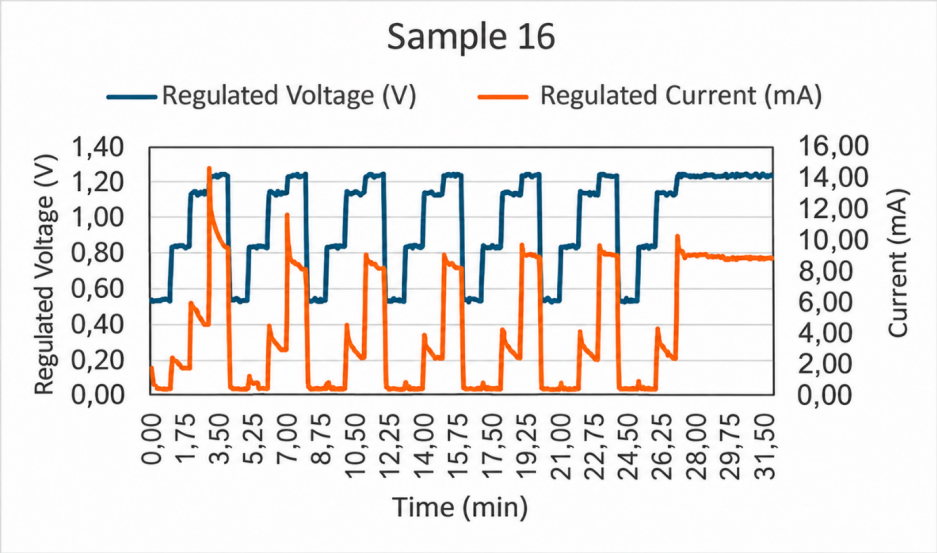

Fig. 10. *Sample 16, with eight cycles, for four voltage levels.*

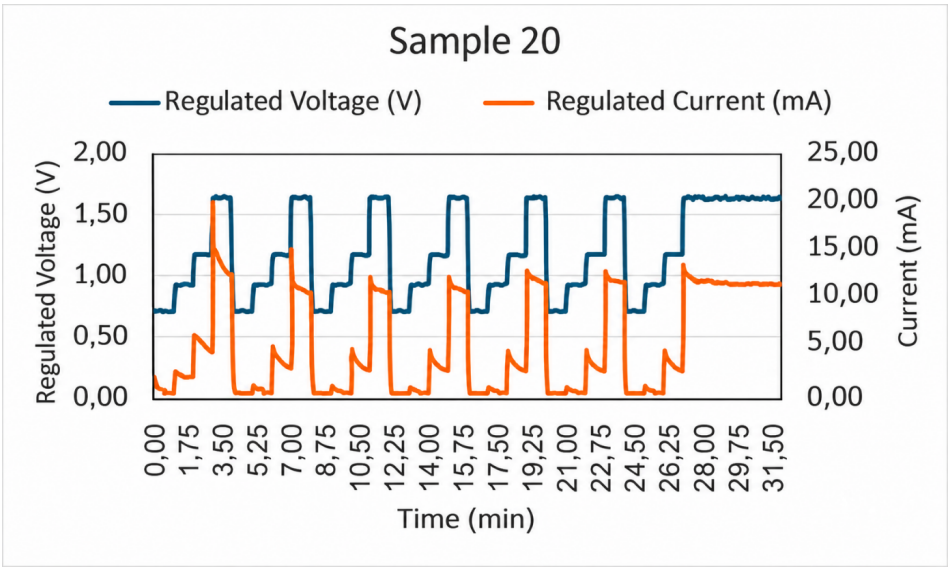

Fig. 11. *Sample 20, with eight cycles, for four voltage levels.*

Each of the samples was weighed before and after the electrodeposition, and their values were recorded in the following table:

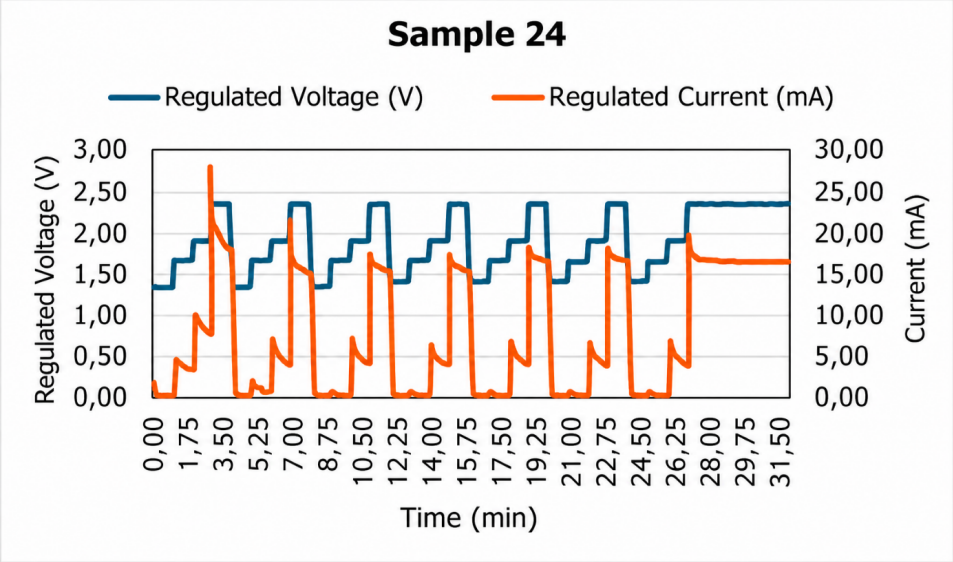

Fig. 12. *Sample 24, with eight cycles, for four voltage levels.*

Sample	Initial mass (g)	Final mass (g)	Mass gain (g)
1	1,18258	1,18302	0,00044
1*	0,77618	0,77664	0,00046
2	0,86377	0,86492	0,00115
2*	0,97453	0,97557	0,00104
3	1,05432	1,05582	0,00150
3*	0,82215	0,82364	0,00149
4	0,94108	0,94358	0,00250
4*	1,12044	1,12302	0,00258
5	0,88763	0,88908	0,00145
5*	0,99231	0,99368	0,00137
6	0,79546	0,79748	0,00202
6*	1,08322	1,08522	0,00200
7	0,91457	0,91692	0,00235
7*	0,85690	0,85911	0,00221
8	1,15438	1,15788	0,00350
8*	0,83312	0,83657	0,00345
9	0,96745	0,96795	0,00050
9*	1,01239	1,01292	0,00053
10	0,78923	0,79063	0,00140
10*	0,87456	0,87594	0,00138
11	1,10231	1,10411	0,00180
11*	0,93412	0,93591	0,00179
12	0,84102	0,84416	0,00314
12*	0,98564	0,98887	0,00323
13	1,06744	1,06925	0,00181
13*	0,81235	0,81414	0,00179
14	0,89945	0,90197	0,00252
14*	1,14238	1,14492	0,00254
15	0,77894	0,78182	0,00288
15*	0,95671	0,95964	0,00293
16	1,03452	1,03902	0,00450
16*	0,86542	0,86995	0,00453
17	0,92218	0,92295	0,00077
17*	1,09874	1,09954	0,00080
18	0,80321	0,80534	0,00213
18*	0,88124	0,88324	0,00200
19	1,17125	1,17400	0,00275
19*	0,94563	0,94834	0,00271
20	1,02347	1,02812	0,00465
20*	0,85231	0,85702	0,00471
21	0,79122	0,79405	0,00283
21*	1,13456	1,13715	0,00259
22	0,90874	0,91253	0,00379
22*	0,97654	0,98023	0,00369
23	1,04562	1,05003	0,00441
23*	0,82945	0,83388	0,00443
24	0,89321	0,89958	0,00637
24*	1,11235	1,11892	0,00657

The data analysis allowed us to determine the mass gain and then, by analyzing the treatments individually by cycles, to plot a comparison of the growth of treatment I versus treatment II (Fig. 13); in this way we found that there is no significant difference between the treatments and that the additional cycle in treatment II adds mass to the electrodes in a regular manner.

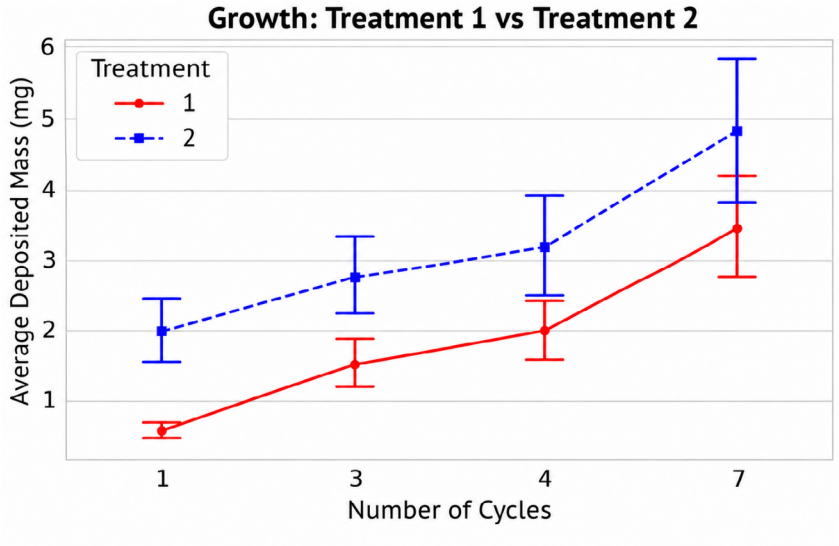

Fig. 13. *Comparison of the average deposited mass for each treatment.*

CONCLUSIONS

The synthesis protocol of the coatings for electrodes, via electrodeposition synthesis, is controllable in terms of voltage and number of cycles.

These results suggest that electrodeposition is a promising technique for the fabrication of electrodes or electronic devices based on nickel sulfide.

The electrodeposition synthesis for stable multi-cycle synthesis shows a decay of the current over time, which indicates that the system is entering a passive state in which the electrodeposition rate decreases.

REFERENCES

[1] K. Richardson et al., "Earth beyond six of nine planetary boundaries", *Science Advances*, vol. 9, núm. 37, sep. 2023, doi:10.1126/sciadv.adh2458.

[2] B. Sakschewski et al., Planetary Health Check 2025 A Scientific Assessment of the State of the Planet. 2025. doi:10.48485/pik.2025.017.

[3] A. O. Oni, K. Anaya, T. Giwa, G. Di Lullo, y A. Kumar, "Comparative assessment of blue hydrogen from steam methane reforming, autothermal reforming, and natural gas decomposition technologies for natural gas-producing regions", *Energy Convers. Manag.*, vol. 254, p. 115245, 2022, doi:10.1016/j.enconman.2022.115245.

[4] N. M Santhosh, S. Gupta, V. Shvalya, M. Košiček, J. Zavašnik, y U. Cvelbar, "Advancing Oxygen Evolution Catalysis with Dual-Phase Nickel Sulfide Nanostructures", *Energy & Fuels*, vol. 39, núm. 2, pp. 1375–1383, ene. 2025, doi:10.1021/acs.energyfuels.4c05182.

[5] Y. Chen et al., "Nickel sulfide-based electrocatalysts for overall water splitting", *International Journal of Hydrogen Energy*, vol. 48, núm. 72, pp. 27992–28017, ago. 2023, doi:10.1016/j.ijhydene.2023.04.023.

[6] R.-C. Li et al., "One-step controlled electrodeposition nickel sulfides heterointerfaces favoring the desorption of hydroxyl groups for efficient hydrogen generation", *Rare Metals*, vol. 43, núm. 9, pp. 4377–4386, 2024, doi:10.1007/s12598-024-02806-6.

[7] Z. Wan et al., "Interface engineering of NiS/NiCo2S4 heterostructure with charge redistribution for boosting overall water splitting", *J. Colloid Interface Sci.*, vol. 653, pp. 795–806, 2024, doi:10.1016/j.jcis.2023.09.117.

[8] S. Haghverdi Khamene, N. van Dalen, M. Creatore, y M. N. Tsampas, "Structural and Electrochemical Evolution of Nickel Sulfides During Alkaline Hydrogen Evolution Reaction", ChemSusChem, dic. 2025, doi:10.1002/cssc.202501880.

[9] C. Lyu et al., "Electrodeposition and Optimisation of Amorphous Ni x S y Catalyst for Hydrogen Evolution Reaction in Alkaline Environment", *Chemistry – A European Journal*, vol. 30, núm. 66, nov. 2024, doi:10.1002/chem.202403030.

[10] P. Wang et al., "Interface Engineering of NixSy@MnOxHy Nanorods to Efficiently Enhance Overall-Water-Splitting Activity and Stability", *Nano-Micro Letters*, vol. 14, núm. 1, p. 120, dic. 2022, doi:10.1007/s40820-022-00860-2.

[11] W. Tan y H. He, "One-step electrodeposition of W, Mo-Ni 3 S 2 /NF catalyst: an efficient hydrogen evolution electrode for alkaline media", *RSC Advances*, vol. 15, núm. 47, pp. 39355–39367, 2025, doi:10.1039/D5RA07318A.

[12] R. Li, P. Kuang, S. Wageh, A. A. Al-Ghamdi, H. Tang, y J. Yu, "Potential-dependent reconstruction of Ni-based cuboid arrays for highly efficient hydrogen evolution coupled with electro-oxidation of organic compound", *Chemical Engineering Journal*, vol. 453, p. 139797, 2023, doi:10.1016/j.cej.2022.139797.

[13] I. A. Poimenidis, M. Lykaki, N. Papakosta, P. A. Loukakos, N. Kallithrakas Kontos, y M. Konsolakis, "One-step electrodeposition of

NiS heterostructures on nickel foam electrodes for hydrogen evolution reaction: On the impact of thiourea content", *Results Chem.*, vol. 6, p. 101216, 2023, doi10.1016/j.rechem.2023.101216.

[14] D. Montgomery y C. St, Design and Analysis of Experiments, 9th Edition. 2022.

[15] D. McKenzie, "Designing and analysing powerful experiments: practical tips for applied researchers", *Fiscal Studies*, vol. 46, núm. 3, pp. 305–322, sep. 2025, doi:10.1111/1475-5890.70003.

[16] C. Miao et al., "Facile Electrodeposition of Amorphous Nickel/Nickel Sulfide Composite Films for High-Efficiency Hydrogen Evolution Reaction", *ACS Appl. Energy Mater.*, vol. 4, núm. 1, pp. 927–933, ene. 2021, doi:10.1021/acsaem.0c02863.

[17] B. Qiao et al., "NixSy/NF composites assembled by sulfidation of nickel foam (NF) for highly effective capture of iodine", *Chemical Engineering Journal*, vol. 479, p. 147864, 2024, doi:10.1016/j.cej.2023.147864.

[18] S. Esmailzadeh, T. Shahrabi, Gh. Barati Darband, y Y. Yaghoubinezhad, "Pulse electrodeposition of nickel selenide nanostructure as a binder-free and high-efficient catalyst for both electrocatalytic hydrogen and oxygen evolution reactions in alkaline solution", *Electrochim. Acta*, vol. 334, p. 135549, 2020, doi:10.1016/j.electacta.2019.135549.

[19] B. Zhong, S. Wan, P. Kuang, B. Cheng, L. Yu, y J. Yu, "Crystalline/amorphous Ni/NixSy supported on hierarchical porous nickel foam for high-current-density hydrogen evolution", *Appl. Catal. B*, vol. 340, p. 123195, ene. 2024, doi:10.1016/j.apcatb.2023.123195.

[20] P. Kotei, N. Boadi, S. Saah, y M. Mensah, "Synthesis of Nickel Sulfide Thin Films and Nanocrystals from the Nickel Ethyl Xanthate Complex", *Advances in Materials Science and Engineering*, vol. 2022, pp. 1–10, jul. 2022 doi:10.1155/2022/6587934.

[21] Y.-K. Hsu, A. Mondal, Y.-Z. Su, Z. Sofer, K. Shanmugam Anuratha, y J.-Y. Lin, "Highly hydrophilic electrodeposited NiS/Ni3S2 interlaced nanosheets with surface-enriched Ni3+ sites as binder-free flexible cathodes for high-rate hybrid supercapacitors", *Appl. Surf. Sci.*, vol. 579, p. 151923, 2022, doi:10.1016/j.apsusc.2021.151923.

ACKNOWLEDGMENTS

To the Universidad de Antioquia, to the TESLA Research Group and to Professor Claudia Patricia Parra Medina for all their contributions.

FUNDING

No financing

CONFLICT OF INTEREST

None

AUTHORSHIP CONTRIBUTIONS

Drafting – original draft: Esteban Quintero Moreno, Héctor Darío Sánchez Londoño, Edwin García Quintero.

Writing–review and editing: Esteban Quintero Moreno, Héctor Darío Sánchez Londoño, Edwin García Quintero.